

Rectification of spatial disorder

Jaegon Um,¹ Hyunsuk Hong,² Fabio Marchesoni,³ and Hyunggyu Park¹

¹*School of Physics, Korea Institute for Advanced Study, Seoul 130-722, Korea*

²*Department of Physics, Chonbuk National University, Jeonju 561-756, Korea*

³*Scuola di Scienze e Tecnologie, Università di Camerino, I-62032 Camerino, Italy*

We demonstrate that a large ensemble of noiseless globally coupled-pinned oscillators is capable of rectifying spatial disorder with spontaneous current activated through a dynamical phase transition mechanism, either of first or second order, depending on the profile of the pinning potential. In the presence of an external weak drive, the same collective mechanism can result in an absolute negative mobility, which, though not immediately related to symmetry breaking, is most prominent at the phase transition.

PACS numbers: 05.60.-k, 05.45.Xt, 64.60.-i

Rectifiers are special devices capable of extracting a steady output signal (current) even from a perfectly center-symmetric input signal (drive) [1]. Their minimal operating conditions typically require an asymmetric internal dynamics, possibly chosen to optimize performance, and a non-stationary unbiased input signal, mostly a cyclostationary periodic drive or a time-correlated noise. In thermodynamical terms, rectifiers are devices that operate under *nonequilibrium* conditions. Direction and magnitude of their output current strongly depend on both the drive(s) (intensity and time scales) and their intrinsic noise (temperature). Rectifiers are often called ratchets or else, to emphasize the role played by fluctuations, Brownian motors [2].

Rectification of an external symmetric signal can be strong enough to overcome the action of an additional static drive, or load, so that the rectifier can do mechanical work against it. Moreover, under appropriate circumstances, the load itself induces an asymmetry in the otherwise perfectly symmetric dynamics of the motor, thus allowing rectification of symmetric ambient fluctuations in a direction that depends on the details of the modified motor dynamics. This mechanism can produce the apparently counterintuitive effect of a spontaneous system response oriented against the load: Rectifiers working under such operating conditions are said to exhibit absolute negative mobility (ANM) [3].

The question now arises whether only time-dependent signals can fuel such rectification mechanisms. To explore the possibility of replacing temporal variability by spatial randomness, we considered an ensemble of N coupled simple phase oscillators, each driven by a static force, randomly chosen to model their interaction with a spatially homogeneous, quenched disordered landscape. Their equilibrium phase values coincide with the local minima of a periodic bistable pinning potential with center-symmetric cells. Following Kuramoto's prescription [5], strong cooperative effects among oscillators are ensured by assuming global pair coupling, irrespective of spatial separation. At finite temperatures and in the limit $N \rightarrow \infty$, this system is known to undergo sponta-

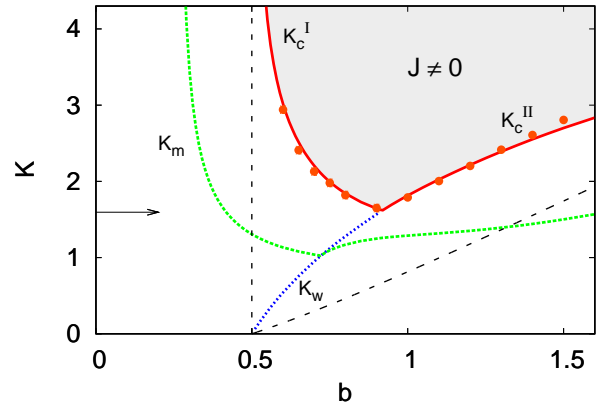


FIG. 1: (Color online) Phase diagram at $f_e = 0$. The thresholds of SSB (K_c), global bistability (K_w), and ANM (K_m), are plotted versus b when $\sigma_\omega = a = 1$. All curves are obtained by analyzing Eqs. (3)-(6) in the mean field approximation. Numerical data (dots) are obtained by integrating Eq. (1) with $N = 10^6$, starting from random initial conditions. Note that the two transition branches (K_c^I and K_c^{II}) are connected by a cusp at $(K^*, b^*) \simeq (1.68, 0.94)$. The dashed curves are the analytic limits of K_c^I and K_c^{II} for $\sigma_\omega = 0$, i.e., $g(\omega) = \delta(\omega)$; the horizontal arrow indicates the critical coupling for the unpinned Kuramoto model, $\sqrt{8/\pi}\sigma_\omega$.

neous symmetry breaking (SSB) [6]. As a consequence, it generates a spontaneous current in either direction; moreover, subjected to an external weak global drive, it can also exhibit ANM and thus work as a motor. Since first detected, both effects have been interpreted as rectification phenomena induced by thermal noise [6, 7].

In this Letter, we show that a large ensemble of noiseless coupled-pinned oscillators is capable of rectifying local forces or stresses, associated with spatially distributed quenched disorder. By numerically analyzing the stationary dynamics of the oscillator ensemble, we demonstrate that the onset of spontaneous rectification currents obeys a dynamical phase transition mechanism, either of first or second order, depending on the degree of bistability of

the pinning potential. Moreover, we observe that ANM is neither induced by thermal noise, nor immediately related to symmetry breaking, although its magnitude is most prominent at the phase transition.

We consider a system of N pinned phase oscillators coupled through the Kuramoto-type global interaction [5],

$$\dot{\phi}_i = \omega_i + f_e - V'(\phi_i) - (K/N) \sum_{j=1}^N \sin(\phi_i - \phi_j), \quad (1)$$

where ϕ_i and ω_i denote, respectively, the phase and the intrinsic frequency of the i -th oscillator. The intrinsic frequencies are assumed to be randomly distributed according to a Gaussian distribution function, $g(\omega)$, with zero mean and variance σ_ω ; a tunable frequency bias is introduced by the external drive f_e . The third and fourth term on the r.h.s. represent the pinning force acting on the i -th oscillator and all-to-all ferromagnetic ($K > 0$) coupling between oscillators, respectively. Due to the global nature of the interactions, mean-field (MF)-type phase transitions are expected.

For simplicity, the pinning potential $V(\phi)$ is chosen to be identical for all oscillators,

$$V(\phi) = -a \cos \phi + (b/2) \cos 2\phi, \quad (2)$$

with $V'(\phi) = dV/d\phi$. $V(\phi)$ is a symmetric biharmonic potential, $V(-\phi) = V(\phi)$, with period 2π . Its unit cells are monostable with one minimum at $\phi = 0 \pmod{2\pi}$ for $b \leq a/2$, and bistable with two stable points at $\phi = \pm\phi_m$ for $b > a/2$, where $\phi_m = \arccos(a/2b)$. Isolated oscillators are symmetrically locked for $|\omega_i + f_e| < f_p$ with locking phases $|\phi_i| < \phi_p$, where the largest locking phase ϕ_p is the (larger) positive solution of the equation $V'''(\phi) = 0$ and the depinning frequency threshold is $f_p = V'(\phi_p)$.

In contrast to Refs. [6, 7], the coordinates ϕ_i are not coupled to a heat bath. As the ergodic assumption does not apply here, the oscillator dynamics can depend on the initial conditions (i.c.), $\{\phi_i(0)\}$. The simulation data reported below refer to the case of disordered i.c., where $\{\phi_i(0)\}$ have been uniformly randomized in the interval $(0, 2\pi)$. We also simulated ordered initial configurations with pinned phases, $\phi_i(0) = \phi_m$, and even annealing procedures. We found that the key qualitative features of our main conclusions do not change.

Following the Kuramoto's approach [5], we introduce the synchronization order parameter Δ and the average phase θ , defined by $\Delta e^{i\theta} \equiv \langle e^{i\phi_j} \rangle$, where $\langle O_j \rangle = (1/N) \sum_{j=1}^N O_j$ denotes the oscillator ensemble average. Accordingly, Eqs. (1) can be rewritten as

$$\dot{\phi}_i = \omega_i + f_e - U'(\phi_i), \quad (3)$$

with the *effective* potential $U(\phi)$ given by

$$U(\phi) = V(\phi) - K\Delta \cos(\phi - \theta). \quad (4)$$

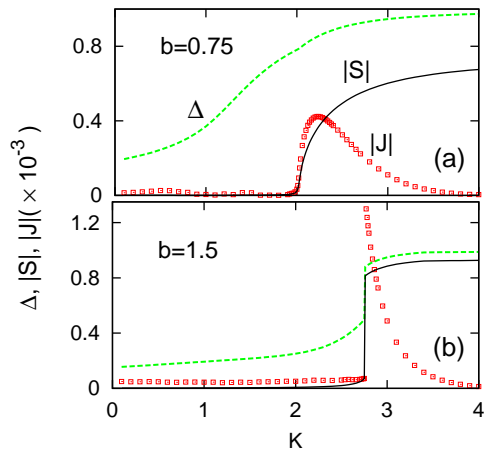


FIG. 2: (Color online) Spontaneous currents. $|J|$ (squares), Δ (dashed) and $|S|$ (solid) versus K (a) in region I at $b = 0.75$, and (b) in region II at $b = 1.5$, from the numerical integration of Eq. (1).

Here, the parameters Δ and θ are determined through the self-consistency relations

$$C = \Delta \cos \theta = \langle \cos \phi_j \rangle = \int \cos(\phi(\omega)) g(\omega) d\omega, \quad (5)$$

$$S = \Delta \sin \theta = \langle \sin \phi_j \rangle = \int \sin(\phi(\omega)) g(\omega) d\omega. \quad (6)$$

For $\theta = 0$, the potential $U(\phi)$ is characterized by the depinning frequency thresholds $\pm\tilde{f}_p$, the corresponding depinning phases $\pm\tilde{\phi}_p$, and, if bistable, the two symmetric minima at $\phi = \pm\tilde{\phi}_m$, similar to the isolated oscillators. The interaction term in $U(\phi)$ tends to suppress the bistability of the pinning potential even for $b > a/2$: $U(\phi)$ is bistable only for small K , $0 \leq K < K_w$, where the bistability threshold K_w is the solution of the implicit equation of $K_w \Delta(K_w) = 2b - a$. For $\theta \neq 0$, $U(\phi)$ is no longer mirror symmetric; correspondingly, the symmetric depinning thresholds, $\pm\tilde{f}_p$, are replaced by two distinct thresholds, $\tilde{f}_p^\pm(K, f_e)$, with $\tilde{f}_p^+ \neq -\tilde{f}_p^-$.

In the absence of external drives ($f_e = 0$), the anti-symmetry of Eq. (3) guarantees $\phi(\omega) = -\phi(-\omega)$ as long as $\theta = 0$, so that the current $J = \langle \dot{\phi} \rangle / 2\pi$ is identically zero. A net SSB current sets on only for $\theta \neq 0$, where two distinct frequency thresholds ($\tilde{f}_p^+ \neq -\tilde{f}_p^-$) break the left-right symmetry of the running oscillators. As the pinning ensures a certain degree of synchronization ($\Delta > 0$ at all $K \geq 0$), the average phase θ alone (or more conveniently S) becomes the proper order parameter of the system. Supersymmetry considerations [1] rule out spontaneous currents for a purely harmonic pinning potential ($a = 0$ or $b = 0$). A biharmonic $V(\phi)$, instead, allows nonzero S and J in the strong coupling regime of $K > K_c$. The transition threshold K_c is actually a function of two parameters only, σ_ω and b , since a can be rescaled to unity

without loss of generality.

To investigate a large ensemble of disordered oscillators, we had recourse to the numerical integration of the equations of motion, Eq. (1), for the entire ensemble. For the sake of a comparison, we also numerically solved the self-consistency equations, Eqs. (3)-(6). In Fig. 1, we compare the dependence of K_c and K_w on the pinning bistability parameter b at $f_e = 0$. The intersection of $K_c(b)$ and $K_w(b)$ at $b = b^*$ defines two distinct dynamical regimes: (i) *region I* ($a/2 < b < b^*$). The SSB transition occurs after the pinning bistability is completely suppressed by the Kuramoto coupling ($K_c^I > K_w$). The transition branch K_c^I diverges as $b \rightarrow a/2$ as expected and decays toward a minimum at $b = b^*$; (ii) *region II* ($b > b^*$). The transition branch K_c^{II} always lies below K_w [8], so SSB occurs inside the bistability regime where multiple solutions are possible. Moreover, we notice that $K_c^I(b)$ and $K_c^{II}(b)$ form a cusp at $b = b^*$, which indicates that two different SSB mechanisms are at work in regions I and II.

Following this lead, we numerically computed the spontaneous current, J , as a function of K at $b = 0.75$ in region I and $b = 1.5$ in region II, see Fig. 2. The difference is revealing: The onset of J can be regarded as a dynamical phase transition of the *second* order, with

$$|J| \propto (K - K_c)^{1/2}, \quad (7)$$

in region I, and of the *first* order, in region II. In the latter, $|J|$ jumps discontinuously from 0 to a maximum at $K = K_c^{II}$, and finally decays exponentially at larger K . Similar continuous or discontinuous behaviors at the transition points are exhibited by the corresponding order parameters Δ and S . No first order transitions were detected in the presence of noise [6].

The existence of a nonzero SSB current for $K > K_c^I$ can be analytically explained in region I by linearizing Eqs. (3)-(6) for small $S \simeq \Delta\theta$. A net current can only result from the oscillators running respectively to the right with $\omega > \tilde{f}_p^+$ and to the left with $\omega < \tilde{f}_p^-$. In the linear regime, it is easy to find from Eqs. (3) and (4)

$$\tilde{f}_p^\pm \simeq \pm \tilde{f}_p + K |\cos \tilde{\phi}_p| S,$$

which yields the net current J for small drive f_e

$$2\pi J \propto -(\tilde{f}_p^+ + \tilde{f}_p^-)/2 \simeq f_e - K |\cos \tilde{\phi}_p| S. \quad (8)$$

Here, Eq. (8) implies a linear response also to the external drive f_e , which will be discussed later. At $f_e = 0$, $J \propto -S$ near the transition.

The critical behavior of S near the transition can be also extracted by linearizing the self-consistency Eqs. (5) and (6) at $f_e = 0$. Since the system has the Ising-like Z_2 symmetry, Eq. (6) is expanded in odd powers of S as

$$S = (K/K_c)S - \kappa S^3 + \mathcal{O}(S^5). \quad (9)$$

With $\kappa > 0$, we find the stable solution of $S = 0$ for $K \leq K_c^I = K_c$ and a new stable branch of $S \propto (K - K_c^I)^{1/2}$ for $K \gtrsim K_c^I$, which determines the MF critical exponent of the current in Eq. (7).

The first order transition along $K_c^{II}(b)$ in region II is a unique feature of our model. It occurs where the static phase solution of Eq. (3) for the locked oscillators consists of two *disconnected* branches, $\phi_{1,2}(\omega)$, with $\phi_1(-\omega) = -\phi_2(\omega)$ in a small ω interval centered around $\omega = 0$. For a homogeneous randomization of the initial phases, both solutions $\phi_{1,2}(\omega)$ contribute to the ensemble averages with statistical weights proportional to the respective basin size. For oscillators with $\omega = 0$, these weights are equal at $\theta = 0$. As θ departs from zero, the symmetry of two branches is broken, but the deterministic nature of dynamics does not allow the system to redistribute the oscillator ensemble across the gap separating two solutions (as it would in the presence of noise [6]). Such a resistance of the system against perturbations reflects itself in a *delayed* onset of the SSB phase in region II; as a consequence, κ becomes negative well before the transition, which causes a discontinuous jump in θ at the transition. Indeed, the SSB transition is delayed until the $S = 0$ solution becomes *locally* unstable (no matter what the global potential shape is, as the oscillators are unable to redistribute themselves between the two basins). Therefore, the transition threshold K_c^{II} is again determined by the linear term in Eq. (9), with the difference that for $\kappa < 0$ (at the transition) the stable solution of S exhibits a discontinuity. This mechanism is distinct from the ordinary first order transition in equilibrium systems.

In the regime of weak disorder, $\sigma_\omega \ll |\tilde{f}_p^\pm|$, the contributions from the running (depinned) oscillators to C and S are negligible. Then, the ensemble averages in Eqs. (5) and (6) can be restricted to static (pinned) oscillators only with $\omega \in (\tilde{f}_p^-, \tilde{f}_p^+)$. In this approximation, we can locate K_c in Eq. (9) very accurately, leading to the curves $K_c^I(b)$ and $K_c^{II}(b)$ drawn in Fig. 1. One may obtain a simpler but less accurate expression for K_c as $1/K_c \simeq \langle \cos^2 \phi / U''(\phi) \rangle$ [9], which becomes exact at $\sigma_\omega = 0$ for identical oscillators [10]. Its solutions exhibit, besides the two diverging branches for $b \rightarrow \infty$ and $b \rightarrow a/2$, also a suggestive lower bound at $b = b^*$ as $\sigma_\omega \sqrt{8/\pi}$, which happens to coincide with the critical coupling of the unpinned Kuramoto model [$V(\phi) \equiv 0$].

The reentrant profile of the transition curve $K_c(b)$ can be explained through a simple qualitative argument. The dynamics of a pinned oscillator in Eq. (1) results from the competition of two opposing forces: (i) the random local drive with typical amplitude σ_ω ; (ii) the Kuramoto coupling, which is enhanced by a bistable pinning potential. For a phase transition to occur, the average attractive Kuramoto force must win over disorder, i.e., $(K/2) \sin 2\phi_m = K(a/2b) \sqrt{1 - (a/2b)^2}$ must be larger than σ_ω . The non-monotonicity of $\sin 2\phi_m$ in the range $0 \leq \phi_m \leq \pi/2$ determines the convexity of $K_c(b)$. In par-

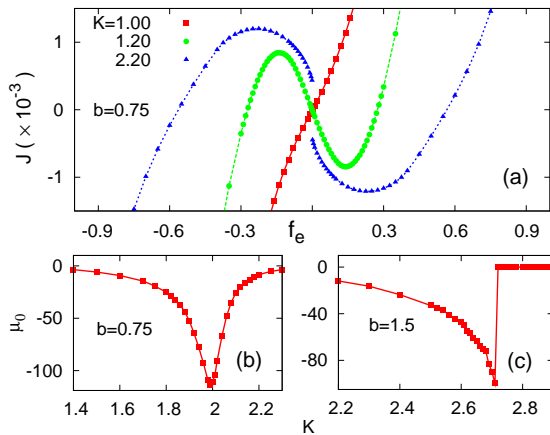


FIG. 3: (Color online) Absolute negative mobility. (a) J - f_e characteristic curve for $b = 0.75$ and three different K from numerical integration of Eq. (1). (b), (c) μ_0 versus K in the vicinity of the transition point for (b) $b = 0.75$, and (c) $b = 1.5$. For graphical convenience, μ_0 has been rescaled by the factor $2\pi/|\phi|$.

ticular, $K_c(b)$ diverges in correspondence with the zeros of $\sin 2\phi_m$, like $\frac{1}{2}(b - a/2)^{-1/2}$ for $b \rightarrow a/2$, and proportional to $2b$ for $b \rightarrow \infty$, in agreement with Fig. 1.

Further evidence of the coexisting phase transitions of the first and second order was obtained by investigating the system response to a finite bias f_e , and more specifically, by analyzing the driven current $J(f_e)$ and its zero-point mobility, $\mu_0 = (dJ/df_e)_{f_e=0}$. We computed both quantities by direct integration of Eq. (1) and summarized our results in Fig. 3. In panel (a), the characteristic curve J - f_e clearly exhibits three different regimes: (1) $0 < K < K_m$. Below a certain threshold K_m (also plotted versus b in Fig. 1), J is parallel to f_e as expected in the linear response theory ($\mu_0 > 0$); (2) $K_m < K < K_c$. The drive modifies the global interaction of the oscillators with their pinning potential in such a fashion that the ensemble response points against the drive. The curve $J(f_e)$ is continuous at $f_e = 0$ with $\mu_0 < 0$ (ANM), and turns positive for larger f_e ; (3) $K > K_c$. The slope of $J(f_e)$ at the origin, μ_0 , can grow so negative that eventually the curve splits into two disconnected antisymmetric branches with $J(0^+) = -J(0^-) < 0$ and uniquely defined negative μ_0 (ANM). This discontinuity is a signature of SSB and is a common feature of both regions I and II. Note that ANM occurs regardless of the presence of thermal noise.

The different SSB mechanisms of regions I and II also influence the ANM properties of the system, see Figs. 3 (b) and (c). In region I, $\mu_0(K)$ develops an asymmetric negative peak numerically compatible with a two-sided divergence for $K \rightarrow K_c^{I\pm}$. In region II, $\mu_0(K)$ is clearly discontinuous with a negative diverging branch for $K \rightarrow K_c^{II-}$, and a slowly decaying one for $K > K_c^{II}$.

In both regions, for exceedingly large or small coupling constants $\mu_0(K)$ tends to vanish, as expected. Finally, we remark that ANM does not necessarily anticipate SSB, as apparent in Fig. 1, where the curve $K_m(b)$ (marking the ANM onset) crosses into a region of the monostable pinning for $b < a/2$, inaccessible to $K_c(b)$.

The numerical results of Fig. 3 can be qualitatively understood from the linear response Eq. (8) for the current, which yields

$$\mu_0 \propto 1 - K |\cos \tilde{\phi}_p| \chi, \quad (10)$$

where $\chi = (dS/df_e)_{f_e=0}$ is the zero-field susceptibility. The curve $K_m(b)$ plotted in Fig. 1 was obtained, indeed, from Eq. (10) and then checked against the numerical integration data from Eq. (1). Note that $K_m(b)$ also develops a minimum (actually a cusp) as it crosses $K_w(b)$. Like in the ordinary equilibrium MF theory, one can find $\chi \propto |K_c - K|^{-\gamma}$ ($\gamma = 1$) near $K = K_c^I$ and, notably, also for $K \lesssim K_c^{II}$, where the local instability occurs around $S = 0$. Therefore, ANM also diverges at SSB transition point with MF susceptibility exponent $\gamma = 1$, which is consistent with our numerical results.

Finally, among the possible applications of our study, we mention the *tug-of-war* between two groups of molecular motors [11]. Indeed, molecular motors running to the right and to the left, due to a Kuramoto type of attraction, can pull polarized filaments in opposite directions. However, to treat mobile motors in space, the interaction topology of our model needs to be modified *ad hoc* [12].

This work was supported by Basic Science Research Program through NRF grant (No.2010-0009697) funded by the MEST. We thank KIAS center for Advanced Computation for providing computing resources.

-
- [1] P. Reimann, Phys. Rep. **361**, 57 (2002).
 - [2] P. Hänggi and F. Marchesoni, Rev. Mod. Phys. **81**, 387 (2009).
 - [3] R. Eichhorn, P. Reimann, and P. Hänggi, Phys. Rev. Lett. **88**, 190601 (2002); L. Machura, *et al.*, Phys. Rev. Lett. **98**, 040601 (2007); D. Speer, R. Eichhorn and P. Reimann, EPL, **79**, 10005 (2007).
 - [4] P. Reimann *et al.*, Europhys. Lett. **45**, 545 (1999).
 - [5] Y. Kuramoto, *Chemical Oscillations, Waves and Turbulence* (Springer, Berlin, 1984); J.A. Acebrón *et al.*, Rev. Mod. Phys. **77**, 137 (2005).
 - [6] J. Buceta *et al.*, Phys. Rev. E **61**, 6287 (2000).
 - [7] S. E. Mangioni, R. R. Deza, and H. S. Wio, Phys. Rev. E **63**, 041115 (2001); M. Kostur, J. Łuczka, and L. Schimansky-Geier, Phys. Rev. E **65**, 051115 (2002); M.A. Zaks *et al.*, Phys. Rev. E **68**, 066206 (2003).
 - [8] In region II, K_w is no longer simply given by the equation $K_w \Delta = 2b - a$, which is valid only at $\theta = 0$.
 - [9] This approximation is good in regime I for any b and in regime II for $b \rightarrow b^*$ and $b \rightarrow \infty$.

- [10] For $\sigma_w = 0$, both branches can be obtained analytically (Fig. 1): K_c^I becomes a vertical line at $b = a/2$ and $K_c^{II} = 2b + (a/4b)(a - \sqrt{a^2 + 32b^2})$.
- [11] For example, see D. Hexner and Y. Kafri, Phys. Biol. **6** 036016 (2009).
- [12] N. Fujiwara, J. Kurths, and A. Díaz-Guilera, Phys. Rev. E **83**, 025101R (2011).